Available online at www.sciencedirect.com
ScienceDirect
Tectonophysics 433 (2007) 53–64
TECTONOPHYSICS
www.elsevier.com/locate/tecto

A grid-search inversion method looking for the best classification of polyphase fault/slip data

Yehua Shan *, Faxiong Gong, Zian Li, Ge Lin

Laboratory of Marginal Sea Geology, Guangzhou Institute of Geochemistry, Chinese Academy of Sciences, Guangzhou City 510640, P.R. China

Received 31 May 2006; received in revised form 19 December 2006; accepted 21 December 2006
Available online 8 January 2007

Abstract

A novel, grid search-based stress inversion method is developed in this paper to find the global minima in the solution region for the classification of fault/slip data into many single-phase subsets. Exhaustively repetitious grid searches are taken to deal with possible local minima, in a departure from existing grid search-based inversion methods. Two stopping rules, to stop at the abrupt change of the objective function or at the least change of the classification, are adopted in the method to look for the best classification. Much calculation time is saved by using a modified version of conventional grid search. The feasibility of this proposed method is demonstrated by applying it to two artificial examples and two real examples. However, enormous time in calculation is still needed in the case of a data set either with a large number of data or for a large number of assigned subsets.

Keywords: Fault/slip data; Polyphase; Classification; Stress inversion; Grid search; Global minima

1. Introduction

For structural geologists, the most important stress analysis method is the inversion of stress (principal directions and stress ratio) from fault/slip data measured at outcrop (Ramsay and Lisle, 2000). This initially assumes the existence of a single tectonic phase recorded by the overall data, despite polyphase fault/slip data being common, in reality, on account of the variability of the stress field through geological time. A recent improvement to this method is its extension, in some elaborate ways, to make it applicable to polyphase fault/slip data. Numerous inversion methods have been developed for this purpose. Among them, many structural geologists prefer a forward scheme (e.g., Anglier, 1979; Hardcastle and Hills, 1991; Sato and Yamaji, 2006b) for simplicity and directness, rather than a numerical scheme (e.g., Huang, 1988; Nemcok and Lisle, 1995; Yamaji, 2000; Shan et al., 2003, 2004; Shan and Fry, 2005). The forward scheme is referred to as grid search. In theory, the continuous parameter space is meshed into a vast number of nodes that are searched exhaustively for the solution of stress.

However, our recent re-examination of grid search strategies provided a modification of the basic method. In Fry's (1999) sigma space, each datum vector has a normal hyperplane centered at the origin for its solution region. For a certain fault/slip data set, many such hyperplanes are superimposed, probably producing a large number of possible solutions that satisfy at least

* Corresponding author. Tel.: +86 20 85290763; fax: +86 20 85290130.
E-mail address: shanyehua@yahoo.com.cn (Y. Shan).

0040-1951/$ - see front matter © 2007 Elsevier B.V. All rights reserved.
doi:10.1016/j.tecto.2006.12.010

four data, the minimum number of data for stress inversion. Amongst these possible solutions there exist many local minima, in addition to meaningless minima defined by fewer than four independent data, if one defines an objective function such as the sum of square distances between the datum vectors and the stress hyperplane (Shan et al., 2003, 2004). The next step is to group the possible solutions into a few meaningful ones, which in this circumstance becomes crucial to the calculation. The important issue arises, of how to make the best grouping. This issue seems to have attracted little attention.

In applying an inversion method to a set of polyphase fault/slip data, the data are eventually classified into single-phase subsets through using some criterion particular to the method. In the numerical methods, iteration is normally undertaken to look for the best classification, but local minima described above are then pitfalls in reaching the global minimum. Not all inversion methods of the numerical type can deal with these local minima, for any given polyphase data set. We believe that this is a major reason why applying the methods to a certain data set may give widely varying results. In relating variation to the reliability of the methods, Liesa and Lisle (2004) never noticed the effect, on the result, of local minima reached at the final iteration.

This communication aims at the development of a novel, grid-search based inversion method in the forward category. The method can find the global minimum, at which the best classification of the data is obtained. This is of the greatest advantage to grid search, but at the cost of enormous time needed in calculation. Meanwhile, Xu (2004) has proposed a numerical algorithm for nearly the same purpose; but this will not be discussed here, as detailed comparison between these two methods is beyond the scope of this paper.

Symbols used in this paper and their definitions are listed in Appendix A.

2. Methodology

Let us classify a set, A, of n fault/slip data into k single-phase subsets, A_i (i=1,2,3...,k). The number of data in each subset is larger than 4, the minimal number of fault/slip data for stress inversion. According to the binominal theorem, there are a tremendous number of combinations for k subsets that must be checked for the best combination, that is to say, for the best classification. Even when k=2, the number would become so large that it is almost impossible to do using the currently fastest personal computer. However, this issue can be resolved by the inversion method proposed below, which is based on grid search.

2.1. Parameter space

In preference to other parameter spaces, reduced sigma space (Fry, 1999), or $[\sigma_{11}, \sigma_{22}, \sigma_{12}, \sigma_{13}, \sigma_{23}]$, is adopted in this paper. It has the advantage that polyphase data may be separated almost in a linear way after some transformation. In the space, fault/slip data of each individual phase are distributed along an independent hyperplane centered at the origin; therefore, polyphase data are readily discriminated into single-phase subsets by recognizing the hyperplanar structures of the overall data in the space (Fry, 1999; Shan et al., 2003, 2004). For more information on sigma space, interested readers are encouraged to read the articles of Fry (1999) and of Shan et al. (2003).

Additionally, Sato and Yamaji (2006a) proved that, in their rescaled full sigma space or $\left[\frac{1}{\sqrt{2}}\sigma_{11}, \frac{1}{\sqrt{2}}\sigma_{22}, \frac{1}{\sqrt{2}}\sigma_{33}, \sigma_{12}, \sigma_{13}, \sigma_{23}\right]$, the Euclidean distance between two stress vectors is equal to the similarity between their corresponding stress tensors (Orife and Lisle, 2003). The two spaces are transformable to each other.

2.2. Mesh

In reduced sigma space, the stress vector is distributed in the hyper-sphere centered at the origin and has a unit-length radius (Fry, 1999; Shan et al., 2003). The hyper-sphere is evenly meshed in order of the first to the fifth element. Hence, the region of the latter element depends upon the values of previous elements as follows:

$$
\begin{aligned}
&[-1, 1] \text{ for } \sigma_{11},\\
&[-\sqrt{1-\sigma_{11}^2}, \sqrt{1-\sigma_{11}^2}] \text{ for } \sigma_{22},\\
&[-\sqrt{1-\sigma_{11}^2-\sigma_{22}^2}, \sqrt{1-\sigma_{11}^2-\sigma_{22}^2}] \text{ for } \sigma_{12},\\
&[-\sqrt{1-\sigma_{11}^2-\sigma_{22}^2-\sigma_{12}^2}, \sqrt{1-\sigma_{11}^2-\sigma_{22}^2-\sigma_{12}^2}] \text{ for } \sigma_{13}, \text{ and}\\
&[-\sqrt{1-\sigma_{11}^2-\sigma_{22}^2-\sigma_{12}^2-\sigma_{13}^2}, \sqrt{1-\sigma_{11}^2-\sigma_{22}^2-\sigma_{12}^2-\sigma_{13}^2}] \text{ for } \sigma_{23}.
\end{aligned}
$$

There are other methods of more even meshing (e.g., Sato and Yamaji, 2006b), but discussion of this is beyond the scope of this paper. No matter how the space is meshed, there still exists a possibility that the unknown controlling stresses are not located at the nodes of the mesh. The misfit, if large, may influence the result of grid searching. In order to overcome this, denser meshes are needed, but this is at the cost of vast memory and computation time. For example, there are 1,589,156 grid points for a mesh width of 0.05.

2.3. Objective function

Like most inversion methods in the numerical category, a criterion must be established by which to search for the solution of stress in the parameter space. This is generally done by optimizing an objective function defined in a way particular to each method. The objective function defined in this paper is the summation of square distances between datum vectors and their corresponding stress hyperplanes in reduced sigma space. It is expressed as follows:

$$F(k,A)=\sum_{i=1}^{k}\sum_{j\in A_i}(t_j b_i^T)^2 \tag{1}$$

where k is the number of subsets, t_j is the j-th fault/slip datum, b_i is the controlling stress vector for the i-th subset or A_i, A is the set of the overall data, $A=\cup_{i=1}^{k} A_i$ and T is the operation of matrix transposition. By minimizing the objective function, we solve for the single-phase subsets and their corresponding stresses.

The objective function mentioned above has been used previously by Shan et al. (2003, 2004) to classify polyphase data both in a hard way and in a soft way. For the sake of simplicity, this paper will only consider hard classification, in which, by definition, each fault/slip datum must not simultaneously be assigned to more than one subset. Hence,

$$A_i \cap A_j = \{\text{null}\} \tag{2}$$

where $i\neq j$.

2.4. Best classification

In the introduction, a concept of "the best classification" is introduced as a precursor to our new inversion method. It is necessary to make a strict definition of this key concept. By the best classification we mean that a certain fault/slip data set is classified into subsets in a way that produces the global minimum of the objective function defined above. Provided that A_i (i=1,2,3,…,k) are single-phase subsets, we have from the above definition a key assumption that the set is classified in the best way into those primary subsets. It can be restated as follows:

$$F_{\min}(k,A)=\sum_{i=1}^{k} F_{\min}(1,A_i) \tag{3}$$

where $F_{\min}$ represents the global minimum of the objective function for A or A_i. Based on this assumption, our new inversion method is developed, as described below.

2.4.1. Two subsets ($k=2$)

This is a simple case where the fault/slip data set (A) consists only of two single-phase subsets (namely, A_1 and A_2), with k=2. Let $A(i)$ (i=4,5,…,$n-4$) stand for whichever subset of i fault/slip data has the minimum objective function, denoted $F_{\min}(1, A(i))$, for a given value of "i". The presumption tells us that one of the subsets $A(i)$, for some unknown i, must be either A_1 or A_2, but gives us no hint which one. The subset $A(i)$ for each value i can be obtained by checking all the nodes in reduced sigma space in the following way.

1) Produce a value associated with each fault/slip datum, as follows. If the stress vector at the node accounts for the slip sense of the datum, calculate the dot product of the datum vector and the stress vector; otherwise, assign a large value.
2) Sort the data into increasing order of associated value.
3) Calculate the sum of squares of these values for the first i sorted data. This sum, $F(1, A(i))$, is the smallest value that any subset of i data, provided they have correct slip sense, can contribute to the objective function at this node, in accordance with Eq. (1).
4) Compare the value of the objective function obtained, $F(1, A(i))$, with the smallest value from all the previous nodes, and
5) If it is smaller, record this smallest value, and record the first i of its associated sorted data. After all nodes have been processed, this gives us the combination of the node, and the corresponding subset $A(i)$ of i data, having globally the least value of objective function, $F_{\min}(1, A(i))$, for the chosen value of i.

Once $A(i)$ is obtained for this value of i, we take into account a complementary subset of A to $A(i)$, which we designate $A(i, n-i)$, where $A(i, n-i)=A(n)-A(i)$. By taking each node in turn, we then find the node giving $F_{\min}(1, A(i, n-i))$, the smallest value of objective function for this subset.

Finally, we look for the smallest summation of $F_{\min}(1, A(i))$ and $F_{\min}(1, A(n)-A(i))$ (i=4,5,…,$n-4$). The two subsets having the smallest sum are considered as the best classification of A, because in the presumption they are either A_1 and A_2, or A_2 and A_1. The principal directions and stress ratio are calculated from the stress vector assigned to each optimal subset. However, because the controlling stress is not always precisely at the node, the optimal subsets sometimes are not A_1 or A_2, but are approximated by them.

In this final step, we disregard cases having either $F_{\min}(1, A(i))$ or $F_{\min}(1, A(n)-A(i))$ larger than some

assigned limit. In these cases, we may resort to meaningful $F_{\min}(1, A(i))$ and $F_{\min}(1, A(n)-A(i))$, for which the sum of the number of data in the subsets is as large as possible.

2.4.2. More than two subsets ($k>2$)

When the data set consists of three single-phase subsets A_i ($i=1,2,3$), the procedure for our proposed inversion method is described below:

a) obtain subset $A(i)$ ($i=4,5,\ldots,n-8$), as in the previous section,
b) calculate the complementary subset of A to $A(i)$, and then determine in the same way a new subset $A(i, j)$ ($j=4,5,\ldots,n-i-4$) having a number of j data in $A(n)-A(i)$, and reaching the minimum objective function or $F_{\min}(1, A(i, j))$,
c) calculate the complementary subset of A to $A(i)$ and $A(i, j)$, that is $A(i, j, n-i-j)=A(n)-A(i)-A(i, j)$, and calculate the minimum objective function $F_{\min}(1, A(i, j, n-i-j))$, and its associated node,
d) look for the smallest summation of $F_{\min}(1, A(i))$, $F_{\min}(1, A(i, j))$, and $F_{\min}(1, A(i, j, n-i-j))$ ($i=4,5,\ldots,n-8$; $j=4,5,\ldots,n-i-4$), at which the three subsets are considered as the best classification, and
e) calculate principal directions and stress ratio from the stress vector assigned to each optimal subset.

So, in a similar way, one can readily compact a general procedure to carry out the method, with the aid of a great number of symbols. Readers would feel distracted by usage of too many symbols. So, this is not done here but left to interested readers.

2.4.3. An unknown number of subsets

Commonly, we have little or no knowledge about how many single-phase subsets there are in a fault/slip data set collected at outcrop. In this situation, the optimal number of subsets has to be determined by mining the data themselves in some way, for example, by comparing the partition coefficient at different division number (Shan et al., 2004). Essentially, this is an old stopping problem in clustering analysis. Despite numerous proposed stopping rules, either empirical or statistical, the problem has never been satisfactorily resolved (Mojena, 1977; Everitt, 1979; Hartigan, 1985).

Two empirical stopping rules are adopted in this paper. One rule is to look for an abrupt change in the objective function (Eq. (3); Shan and Fry, 2005) for varying assigned number of subsets, at which the optimal subsets are considered the best classification of the data set. Much care is needed in determining the change, since only a small number of assigned subsets, 5 in this paper for instance, is taken into account. It is worth noting that the objective function decreases with the increase of the assigned number of subsets. It is difficult to make the determination if this decrease is smooth or gradual.

Another stopping rule is to look for the best classification as the one having the least change with the increase of assigned number of subsets. This is based upon the belief that the best classification should have the least difference from the classification having one more assigned number of subsets, because it has reached the global minimum. The concept of stress difference (Orife and Lisle, 2003) is borrowed to quantify the difference between two neighboring classifications. For a certain subset, the variation of it is manifest by the minimum difference in stress between it and any of the subsets in the next classification.

2.5. Modified grid search

In the proposed inversion method, grid search is exhaustively repeated in order to look for the optimal subsets such as $A(i)$, $A(i, j)$, and so forth. This is different from pre-existing inversion methods (e.g., Hardcastle and Hills, 1991) that make grid search only once. Accordingly in the proposed method, much more time will be taken in calculation. Due to the nearly exponential increase of optimal subset with number of subsets, the time may become so enormous that it may be beyond the capacity of a computer.

The low efficiency of conventional grid search lies in having to consider a vast number of nodes away from the solutions. Any reduction of nodes would save time in calculation, to a greater or lesser degree. Taking D_{limit} to be the upper distance limit, possible solution nodes are obtained in the following way:

1) for a certain node, compare the calculated and the observed slip senses for each fault/slip datum,
2) calculate the dot product of the stress vector and every fault/slip datum vector with matching slip sense,
3) count the number of data that have a smaller dot product than D_{limit}, and
4) accept the node as one possible solution if the number of acceptable faults is greater than 4.

One may confine grid search to these possible solution nodes. This saves a vast time in calculation (Fig. 1) at almost no cost of accuracy. In this, the value of D_{limit} becomes critical. The smaller their values, the smaller number of possible solution nodes and hence

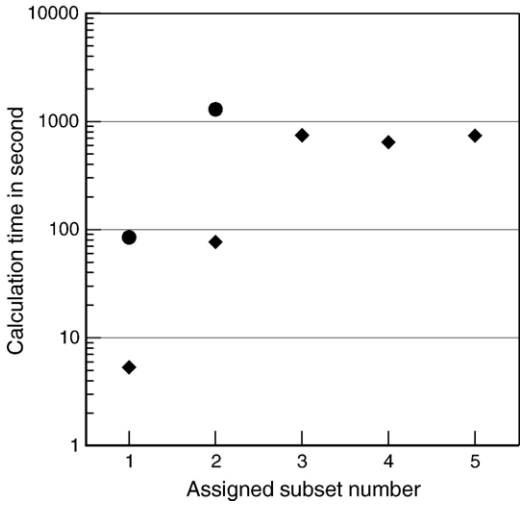

Fig. 1. The calculation time for differing assigned number of subsets, using conventional (filled circles) and modified (filled diamonds) grid search, for an artificial data set taken from Shan et al. (2003). In the latter, the calculation time shown does not include the time of finding possible solution nodes. Mesh width is 0.05. PC used has an Intel Pentium 1.73 GHz CPU, and a 512 MB RAM.

less calculation time, but increased possibility of rejecting solution nodes. Herein lies the problem about the optimal value of D_{limit}, that has the smallest number of possible solution nodes without any loss of accuracy. It is difficult to resolve this problem with little knowledge of the best classification in common cases. The optimal value seems to depend upon the mesh, and the fault/slip data. In this paper, the upper distance limit is set to 0.05, close or similar to the mesh width used.

In addition, it is not necessary to take all the optimal subsets into consideration. For a set of polyphase fault/slip data, the best subsets $A(i)$ obtained by using the proposed method corresponds to the homogeneous subsets having the largest data number, as Eq. (3) implies. Each subset $A(i)$ need only be searched for amongst the best subsets that have at least the mean data number of data per subset. Likewise, following subsets may be sought amongst only those having the least the mean number for the remaining data. This makes it possible to avoid calculating all the best subsets. Take $A(i)$ $(i=4,5,\ldots,n-1)$ for example. Given k to be the maximum assigned number of subsets, we have a mean number of $[n/k]$ data in the best subset obtained through using the proposed method. Only best subsets such that $A(i)$ $(i=[n/k],\ [n/k]+1,\ldots,n-4(k-1))$, need be sought. In an almost identical way, we can deal with $A(i,j)$, $A(i,j,k)$ and so forth.

A computer program was written in the Fortran language to carry out the proposed method, and applied to data sets shown below in this paper.

3. Test of the proposed method

Two artificial fault/slip data sets (Fig. 2), one polyphase and one randomized, are used to demonstrate the feasibility of the proposed inversion method. These data sets are so well-controlled that any calculated classification can be compared with the prescribed

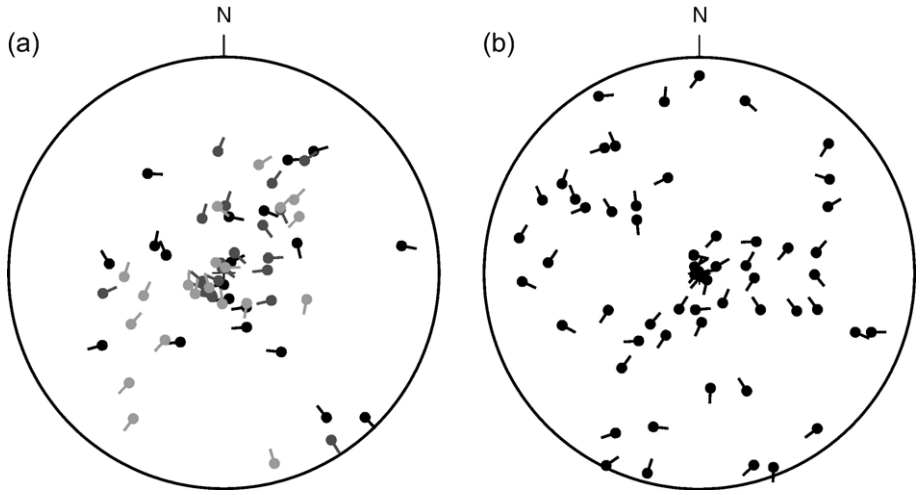

Fig. 2. Lower-hemisphere, equal-area projection of two artificial sets, polyphase (a) and randomized (b). Fault/slip data are represented by the fault dip directions (filled circles) and the slip directions of the hangingwalls (thick short lines). For the former set, subset 1, 2 and 3 are in dark, deep gray, and gray color, respectively.

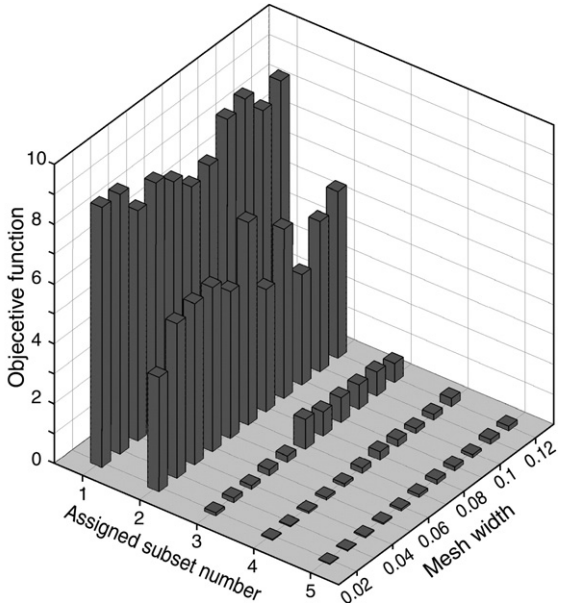

Fig. 3. The variation of the objective function with mesh width and with assigned number of subsets for the artificial polyphase data.

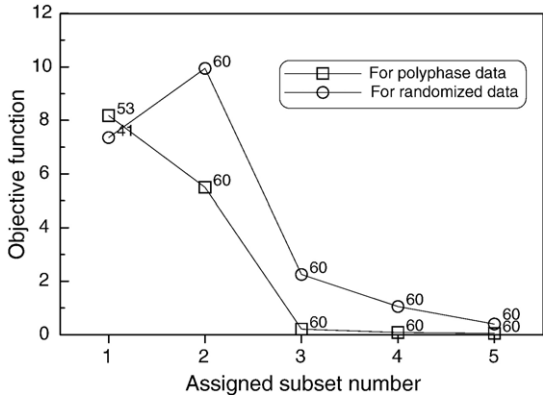

Fig. 5. The variation of the objective function with assigned number of subsets for the polyphase data and for the randomized data. Overall numbers of data in subsets are displayed near the symbols. Mesh width is 0.05.

classification. That is why artificial data are chosen in this section, instead of real data in which controlling stresses are commonly unknown.

3.1. Polyphase set

The first artificial set (Fig. 2a; Appendix B) consists of 60 fault/slip data, in which three single-phase subsets are equally mixed. In each subset, data are evenly generated under a certain prescribed stress, and are not affected by any measurement error. Results of applying the method to the data set are shown in Figs. 3–6a, and listed in Tables 1 and 2.

In Figs. 3 and 5, there exists an abrupt change of the objective function for an assigned number of subsets of 3, even though mesh width is varied from 0.02 to 0.12. For an assigned number of subsets of 3 and at a mesh width of 0.02 or 0.05, the calculated stresses are almost identical to the controlling stresses, and so are the data classifications (Tables 1 and 2). Meanwhile, there is the least change of classification for an assigned number of subsets of 3 (Fig. 6a). These indicate the validity of the proposed

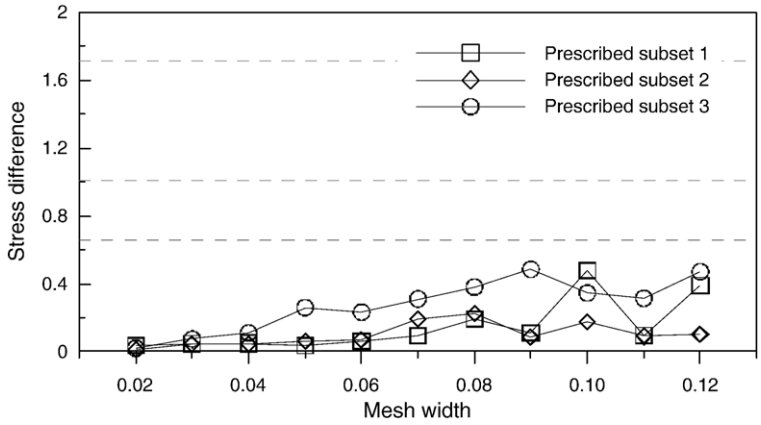

Fig. 4. For an assigned number of subsets of 3, the differences between the calculated and the prescribed stresses. Gray dashed lines represent the boundary values between the different classes of stress difference named by Orife and Lisle (2003), as follows. Two stresses are considered “very similar” if their difference is less than 0.66, “similar” if in a range of 0.66 to 1.01, “different” if in a range of 1.01 to 1.71, or “very different” if greater than 1.71 (Orife and Lisle, 2003). See the text for more explanation.

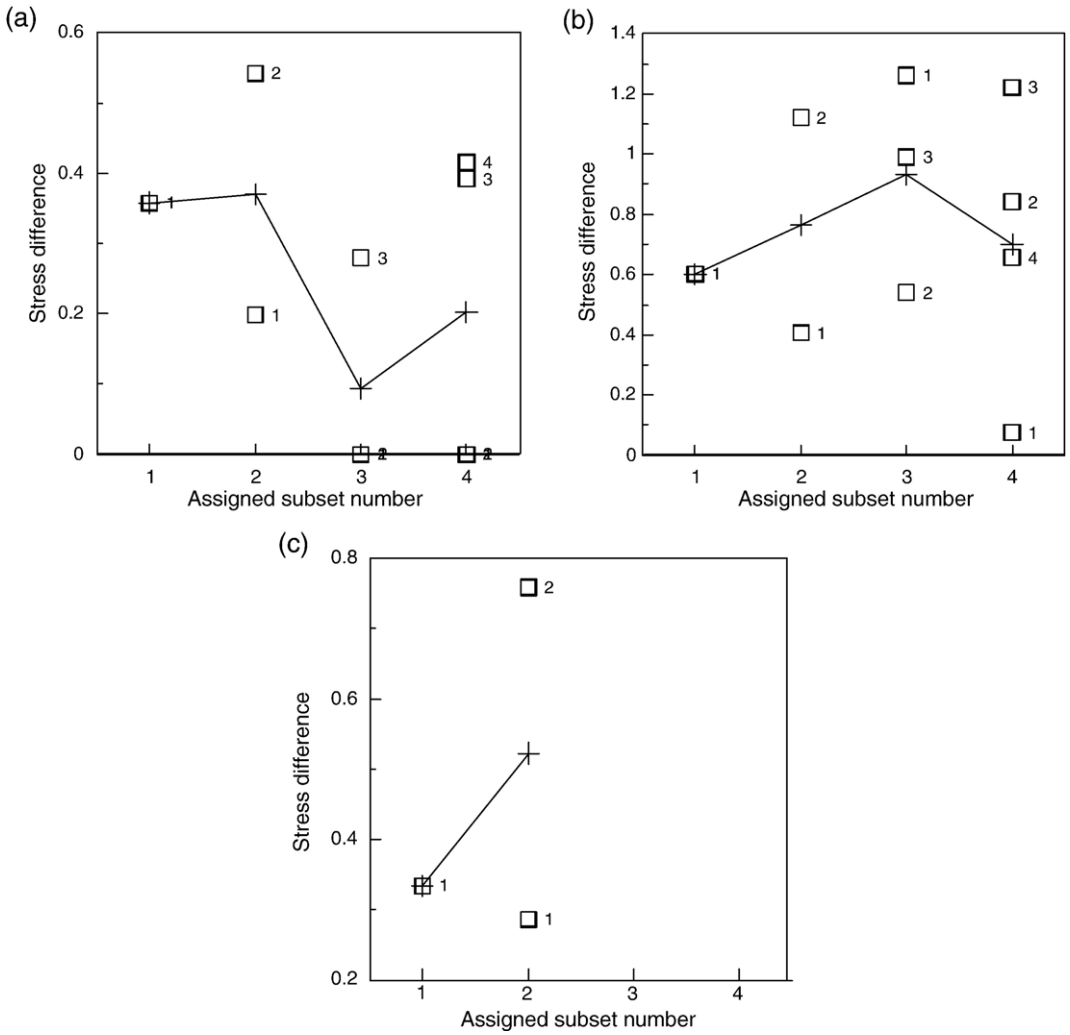

Fig. 6. Stress difference between two neighboring classifications for polyphase data (a), randomized data (b), and Chichi data (c). For a certain calculated stress, the difference is referred to as the smallest difference between it and the calculated stresses in next classification. The geometric mean ("+") of stress differences for each assigned number of subsets is linked by a zig-zag line. Calculated stresses for an assigned number of subsets less than 5 are listed in Tables 1, 3 and 4. See the text for more explanation.

method in separating the polyphase data set into its three best subsets.

The calculated and the prescribed stresses need to be matched in some way to make detailed comparison between them. This is readily done by visually matching two stresses, if they are similar. But it becomes a great problem if two stresses are not similar. Instead, an objective way used in this paper is to match two stresses only if they have very small difference. The similarity or difference between two stress tensors can be quantitatively characterized by the concept of stress difference (Orife and Lisle, 2003). Fig. 4 shows the difference at varying mesh width between the calculated and the prescribed stresses. The calculated stress starts to fluctuate greatly from the first controlling stress at a mesh width of greater than 0.05, and begins to deviate from the third controlling stress at a mesh width of no less than 0.10. In contrast, the second controlling stress remains similar in range to the controlling stress. For this example, using a mesh width of 0.02 to 0.12, stress difference remains less than 0.77, indicating the high accurate estimation of all controlling stresses.

For all mesh widths concerned, the third controlling stress is less accurately estimated than either the first or the second stress, and the first controlling stress tends to be the most accurately estimated. The similarity among

Table 1
A list of prescribed stresses and calculated stresses from the polyphase data set

Phases		Subset	Number of data	Principal directions (°)						Stress ratio	Objective function
				Maximum		Intermediate		Minimum			
				Bearing	Plunge	Bearing	Plunge	Bearing	Plunge		
Pres.		1	20	180.00	10.00	89.00	5.65	329.93	78.48	0.667	0.00
		2	20	140.00	5.00	235.00	44.89	45.04	44.67	0.667	
		3	20	100.00	1.00	195.00	78.67	9.80	11.28	0.667	
Calc.	1	1	53	132.19	6.57	228.10	41.77	34.98	47.48	0.779	4.20
	2	1	51	144.68	6.86	239.88	37.02	45.78	52.13	0.792	3.00
		2	9	268.87	21.19	87.51	68.80	178.69	0.46	0.546	
	3	1	26	141.13	6.59	237.20	42.48	44.07	46.77	0.639	0.10
		2	18	180.06	10.96	88.85	6.19	329.91	77.38	0.663	
		3	16	98.27	0.00	180.00	90.00	8.27	0.00	0.646	
	4	1	26	141.13	6.59	237.20	42.48	44.07	46.77	0.639	0.04
		2	18	180.06	10.96	88.85	6.19	329.91	77.38	0.663	
		3	11	102.88	8.15	223.58	74.33	10.94	13.29	0.686	
		4	5	90.00	0.00	180.00	90.00	0.00	0.60	0.852	

Calculated stresses are made through applying the proposed inversion method to the set at a mesh width of 0.05. Stress ratio is referred to as $(\sigma_1-\sigma_2)/(\sigma_1-\sigma_3)$, where σ_1, σ_2 and σ_3 are the relative magnitudes of the maximum, the intermediate and the minimum principal stresses. Compressional stress is positive in sign, and tensional stress negative in sign. See the text for more explanation.

the controlling stress vectors has been considered as an influence on the accuracy of stress estimation (Shan et al., 2003). However, it is evidently not the unique factor accounting for the variable accuracy, and one should consider other factors, such as the way sigma space is meshed.

Given a certain assigned number of subsets, the objective function has a strong tendency of increasing with decrease in mesh width (Fig. 3). It fluctuates slightly at places, particularly at a large mesh width. This is ascribed to the mesh effect on the solution. In this case, which has definite solutions, decreasing the mesh width does not always leave these solutions closer to nodes in sigma space.

Table 2
Comparison between the estimated and the prescribed stresses

Calc.		Pres.					
		Number of data			Stress difference		
		1	2	3	1	2	3
A	1	20	1	6	0.038	1.074	1.626
	2	0	18	1	1.048	0.013	1.233
	3	0	0	13	1.625	1.226	0.019
B	1	19	2	5	0.035	1.055	1.627
	2	0	18	0	1.007	0.064	1.242
	3	0	1	17	1.697	1.365	0.026

The estimated stresses for a number of subsets of 3 are obtained at a mesh width of 0.02 (A) and 0.05 (B). See Orife and Lisle (2003) for the definition of stress difference between two stress tensors. The parameter is in a range of 0 to 2, and increases with the decrease of their similarity.

3.2. Randomized set

For comparison with the polyphase data set, a randomized data set was stochastically generated under no prescribed controlling stress. It also consists of 60 fault/slip data (Fig. 2b). In the set, fault dip directions are sampled in a range of 0° to 359°, and fault dip angles in a range of 0° to 90°. The pitch of the slip on the fault planes is sampled in a range from down dip minus 90° to down dip plus 90°. Each such slip is assigned at random either with normal sense or with reverse sense. Application of the proposed method gives results in Figs. 5 and 6b, and Table 3.

In Fig. 5, for an overall number of data of 60, the objective function is greater for randomized data than for polyphase data, indicating that the former is either more dispersed or more heterogeneous (that is, polyphase) than the latter. There exists a similar abrupt change of the objective function at an assigned number of subsets of 3. But, its corresponding classification is not the least change (Fig. 6b), thus not allowing us to accept an optimal number of three subsets for the data. When the assigned number of subsets becomes larger, the change of classification tends to decrease. This hints at the much greater heterogeneity of the data.

For an assigned number of subsets of 4, the first subset remains the most stable. Although they are produced under no prescribed stress, we could be inclined to believe that data in the subset have the feature of a single phase. This artifact is probably due to

Table 3
Calculated stresses from the randomized data set using the proposed inversion method at a mesh width of 0.05

No	Subset	Number of data	Principal directions (°)						Stress ratio	Objective function
			Maximum		Intermediate		Minimum			
1	1	41	229.51	3.57	324.21	52.73	136.81	37.04	0.674	7.36
2	1	40	33.88	11.00	292.20	46.17	133.86	41.74	0.928	9.94
	2	20	225.67	73.74	108.19	7.67	16.23	14.26	0.051	
3	1	27	30.83	3.50	135.07	76.03	299.99	13.50	0.684	2.25
	2	21	328.03	79.06	80.29	4.19	171.04	10.09	0.892	
	3	12	156.20	1.16	246.77	26.42	63.87	63.55	0.504	
4	1	21	18.99	13.86	109.11	0.50	201.13	76.13	0.017	1.05
	2	20	252.81	11.36	119.74	73.60	345.19	11.66	0.542	
	3	13	335.82	32.86	127.47	53.73	236.80	13.65	0.202	
	4	8	274.71	75.12	100.14	14.82	9.78	1.35	0.532	

Notation and sign conventions as for Table 1.

the relatively small number of data considered in this case.

4. Applications

The proposed inversion method was applied to two real examples, Chichi fault data (Lee et al., 2003) and Altyn Tagh fault data (Xie and Liu, 1989).

4.1. Chichi fault data

This example is taken from Lee et al. (2003), as modified by Blenkinsop (2006). It consists of 93 fault/slip data from the active Chelungpu fault, a large thrust dipping toward the east in western Taiwan. These surface rupture data had been produced during the 1999 Chichi earthquake along the fault (Lee et al., 2002, 2003; Angelier et al., 2003). All observed slip senses are reverse.

Table 4 lists the results of applying the proposed method to the data set. Stresses are calculated only for an assigned number of subsets of 1 to 3, due to the enormous time in calculation. They vary to a great degree with the assigned number of subsets (Fig. 6c), reflecting the heterogeneous nature of the data. However, there is a very slight stress difference for the first subset between when the assigned number of subsets is 2 and when it is 3. Most likely, this indicates the presence of a single phase recorded by the subset, in spite of the upper limit of 3 subsets. Calculated maximum principal direction (Table 4) is approximately horizontal and E–W trended.

In addition, stress inversed from focal mechanisms in the region (Kao and Angelier, 2001) has no apparently good counterpart among these calculated stresses (Table 4). This misfit may be ascribed to asynchronous slip everywhere along the fault (e.g., Price, 1988; Gutscher et al., 1996), or to heterogeneous distributions of shear stress drop over a large area of the rupture surface (e.g., Day et al., 1998), or to other possible reasons.

4.2. Altyn Tagh fault data

This example consists of 198 fault/slip data that Xie and Liu (1989) collected at the central Altyn Tagh transcurrent fault on the northwest of the Tibetan plateau. Xie and Liu (1989) recognized two distinctive phases, an

Table 4
Calculated stresses from the Chichi data set using the proposed inversion method at a mesh width of 0.05

No	Subset	Number of data	Principal directions (°)						Stress ratio	Objective function
			Maximum		Intermediate		Minimum			
			295	4	28	35	199	54	0.29	
1	1	93	337.01	3.43	246.46	8.97	87.71	80.38	0.107	9.11
2	1	68	91.62	18.91	0.61	2.96	262.05	70.84	0.832	2.96
	2	25	324.23	12.55	233.74	2.21	133.93	77.25	0.268	
3	1	56	93.69	27.32	356.31	13.97	242.09	58.76	0.888	1.32
	2	21	152.75	10.12	62.19	3.11	315.30	79.40	0.083	
	3	16	182.72	7.38	274.94	16.64	69.64	71.71	0.679	

For comparison, stress inversed from focal mechanisms in the region by Kao and Angelier (2001) is also shown at the first row. Notation and sign conventions as for Table 1.

Table 5
Calculated stresses from the Altyn Tagh fault data set using the proposed inversion method at a mesh width of 0.04

Scheme	No	Subset	Number of data	Principal directions (°)						Stress ratio
				Maximum		Intermediate		Minimum		
This paper	1	1	198	80.27	16.95	204.90	61.79	343.26	21.84	0.20
	2	1	179	80.27	16.95	204.90	61.79	343.26	21.84	0.20
		2	19	113.91	29.59	315.67	58.56	209.47	9.68	0.84
FCA	1	1	198	53.4	9.3	144.4	5.7	265.6	79.1	0.68
	2	1	99	166.7	0.7	256.9	16.1	74.5	73.9	0.60
		2	99	72.2	4.2	230.7	85.5	342.0	1.7	0.99
QS	2	1		354.28	43.53	115.19	28.40	225.89	33.17	0.90
		2		65.02	3.55	161.02	59.32	332.93	30.43	0.65

For comparison, stresses inversed from fuzzy clustering analysis (FCA; Shan et al., 2004) and from the quartimini strategy (QS; Shan et al., 2006) are shown below.

earlier N–S compression and a later E–W compression, from the data set and other geological observations. In accordance with their study, Shan et al. (2004) found out that the calculated partition coefficient is maximal for an assigned number of subsets of 2, implying that the data set should be separated into two single-phase subsets.

Listed in Table 5 are stresses calculated using the method proposed here, fuzzy clustering analysis (FCA; Shan et al., 2004) and the quartimini strategy (QS; Shan et al., 2006), respectively. Calculated stresses vary to more or lesser degree with the adopted inversion methods, which in turn illustrates the presence of many local minima in the parameter space that are pitfalls for certain methods. This illustrates the point that it is not good to appraise methods that may not reach the global minimum at all times, on the basis of similar or identical fault data. However, stresses calculated by using the proposed method are roughly similar to those by using FCA. Just notice the similarity between the first subset of this paper and the second subset of the FCA. This suggests that FCA might be better than QS for this example.

In Table 5, for an assigned number of subsets of 1, the stress shown in the category of FCA is obtained as an analytical solution by using the moment method (Fry, 1999; Shan et al., 2003). Its misfit with the stress by using the method developed in this paper is attributed to the inaccuracy of stress solution caused by the discretization of the parameter space. Much more accurate stress would be obtained if finer mesh were adopted, as noted in the second section.

5. Discussions and conclusions

For a given set of measured fault/slip data, there probably exist a number of local minima in the solution region. These local minima become pitfalls for many existing inversion methods in the numerical category that cannot reach the global minima at all times. A novel grid search-based inversion method is developed in the paper for this purpose. It reaches the global minima by means of exhaustively repetitious grid search, and looks for the best classification of the data set into many single-phase subsets, by adopting some stopping rules, to stop at the abrupt change of the objective function or at the least change of the classification. A modified scheme of conventional grid search is taken in order to save time in calculation. The feasibility of this proposed method is demonstrated by its application to examples, two artificial and two real.

However, the main disadvantage of the proposed method is the vast time in calculation, although some measures are taken to reduce this problem. The time increases greatly with either increase in the number of data or increase in the assigned number of subsets. This makes it impossible for users running a personal computer to deal with a data set either with any greater number or for any greater assigned number of subsets.

Without any prior knowledge about controlling stress, it is difficult to determine the number of single-phase subsets in a certain data set. This old problem has not yet been satisfactorily resolved by the adoption of the two stopping rules in this method. This awaits much further study.

Acknowledgements

This work is funded by the Hundred Talent Program of Chinese Academy of Sciences (KZCX0543081001), and the National Natural Science Foundation of China (Grant 40672144). We are greatly indebted to Norman Fry who read the first draft of this manuscript, and made numerous modifications of it, and Tom Blenkinsop who provided the Chichi data in a ready to use format. We also thank R. J. Lisle, editor Jean-Pierre Burg, and one anonymous referee who reviewed this manuscript, and made valuable suggestions and substantial improvements of it.

Appendix A

A list of symbols and their definitions

Symbols	Definitions	Comments
σ_{ij}	Stress components.	$\sigma_{ij}=\sigma_{ji}$, $i, j=1,2,3$.
n	Number of fault/slip data in a set.	
k	Assigned number of subsets, or number of single-phase subsets.	
$[n/k]$	The integer of n/k.	
A or $A(n)$	A set of n fault/slip data, $A=A(n)$.	Eq. (2).
A_i	A single-phase subset.	$i=1,2,\ldots,k$.
$A(i)$	A subset of i data that has the minimum objective function.	$i=4,5,\ldots,n$.
$A(i, n-i)$	$A(i, n-i)=A(n)-A(i)$.	$i=4,5,\ldots,n-4(k-1)$.
$A(i, j, n-i-j)$	$A(i, j, n-i-j)=A(n)-A(i)-A(i, j)$.	$i=4,5,\ldots,n-4(k-1)$; $j=4,5,\ldots,n-i-4(k-2)$.
$F(k, A)$	The objective function for k subsets.	Eq. (1).
$F_{\min}(k, A)$ or $F_{\min}$	The global minimum objective function for k subsets.	Eq. (3).
$F_{\min}(1, A(i))$	The minimum objective function for subset $A(i)$.	
t_j	The j-th fault/slip datum.	Eq. (1).
b_i	The controlling stress vector for subset A_i.	Eq. (1).
D_{limit}	The upper distance limit.	0.05 set in the paper.
T	The operation of matrix transposition.	

Appendix B

A list of 60 polyphase fault/slip data. They are generated under three prescribed stresses and without any measurement errors. Each single-phase subset has a data number of 20. The prescribed stresses of phases 1–3 are shown in the 1st–3rd rows of Table 2. The slip kind is 1 if there is a normal component of relative slip movement in the fault surface, and 2 if there is a reverse component

Phase 1					Phase 2					Phase 3				
Fault planes (°)		Slips (°)		Slip kinds	Fault planes (°)		Slips (°)		Slip kinds	Fault planes (°)		Slips (°)		Slip kinds
Dip direction	Dip angle	Bearing	Plunge		Dip direction	Dip angle	Bearing	Plunge		Dip direction	Dip angle	Bearing	Plunge	
0.01	4.88	352.62	4.84	2	219.41	25.61	232.62	25.02	1	345.08	82.22	73.43	11.85	1
216.49	63.08	163.70	49.98	2	215.84	57.66	145.35	27.82	2	40.88	60.53	314.44	6.26	1
348.46	10.93	353.22	10.90	2	177.26	50.61	112.87	27.76	2	224.01	42.27	134.42	0.37	1
185.39	23.45	191.65	23.33	2	25.80	11.06	9.24	10.61	2	221.06	35.99	136.76	4.13	1
94.65	48.03	57.63	41.60	2	80.50	51.29	155.61	17.78	2	54.33	14.77	99.74	10.49	2
32.24	34.08	354.25	28.07	2	30.23	10.45	12.47	9.96	2	287.62	36.37	281.51	36.22	2
209.60	54.05	177.22	49.35	2	222.01	35.39	244.12	33.35	1	322.79	15.77	278.54	11.43	2
213.09	30.78	202.06	30.31	2	266.15	18.31	353.26	0.96	2	71.26	15.69	93.39	14.59	2
315.59	84.32	226.99	13.77	1	157.98	24.33	105.99	15.56	2	142.69	5.50	213.72	1.79	1
261.44	75.15	190.82	51.39	2	327.20	82.89	237.86	5.29	2	233.31	39.24	314.60	7.05	2
106.96	25.22	66.00	19.58	2	207.74	9.43	223.05	9.11	1	45.03	8.70	73.05	7.69	2
323.82	40.77	6.06	32.55	2	251.47	19.56	176.76	5.36	1	31.99	71.60	307.39	15.82	1
324.55	74.06	51.78	9.63	2	164.08	4.37	225.06	2.12	1	194.63	2.44	179.48	2.36	1
59.30	59.09	344.95	24.26	2	46.37	10.05	23.06	9.25	2	197.99	47.31	147.35	34.51	1
326.46	17.10	351.50	15.57	2	159.04	2.14	215.42	1.18	1	174.44	27.74	220.48	20.05	1
337.05	24.50	355.60	23.36	2	181.50	27.87	108.58	8.83	2	2.61	12.86	84.20	1.91	1
111.04	30.99	101.31	30.62	2	208.45	42.39	125.63	6.51	2	74.23	34.85	115.16	27.75	2
142.35	52.17	183.13	44.28	2	33.63	3.82	22.16	3.75	2	41.40	37.20	312.51	0.84	1
248.09	32.97	256.31	32.71	2	299.77	22.94	346.82	16.09	2	61.25	44.27	131.54	18.20	2
213.27	5.37	152.69	2.65	1	68.71	9.52	39.83	8.35	2	87.85	41.66	107.80	39.91	2

References

Angelier, J., Lee, J.C., Hu, J.C., Chu, H.T., 2003. Three-dimensional deformation along the rupture trace of the September 21st, 1999, Taiwan earthquake: a case study in the Kuangfu school. Journal of Structural Geology 25, 351–370.

Anglier, J., 1979. Determination of the mean principal stresses for a given fault population. Tectonophysics 56, T17–T26.

Blenkinsop, T., 2006. Kinematic and dynamic fault slip analyses: implications from the surface rupture of the 1999 Chi-Chi, Taiwan, earthquake. Journal of Structural Geology 28, 1040–1050.

Day, S.M., Yu, G., Wald, D.J., 1998. Dynamic stress changes during earthquake rupture. Bulletin of the Seismological Society of America 88, 512–522.

Everitt, B.S., 1979. Unresolved problems in cluster analysis. Biometrics 35, 169–181.

Fry, N., 1999. Striated faults: visual appreciation of their constraint on possible palaeostress tensors. Journal of Structural Geology 21, 7–22.

Gutscher, M.A., Kukowski, N., Malavieille, J., Lallemand, S., 1996. Cyclical behavior of thrust wedges: insights from high basal friction sandbox experiments. Geology 24, 135–138.

Hardcastle, K.C., Hills, L.S., 1991. Brute3 and Select: QuickBasic 4 programs for determination of stress tensor configurations and separation of heterogeneous populations of fault slip data. Computer & Geosciences 17, 23–43.

Hartigan, J.A., 1985. Statistical theory in clustering. Journal of Classification 2, 63–76.

Huang, Q., 1988. Computer-based method to separate heterogeneous sets of fault-slip data into subsets. Journal of Structural Geology 10, 297–299.

Kao, H., Angelier, J., 2001. The Chichi earthquake sequence, Taiwan: results from source parameter and stress tensor inversions. Earth and Planetary Sciences 333, 65–80.

Lee, J.C., Chu, H.T., Angelier, J., Chan, Y.C., Hu, J.C., Lu, C.Y., Rau, R.J., 2002. Geometry and structure of northern surface ruptures of the 1999 Mw=7.6 Chi-Chi, Taiwan earthquake: influence from inherited fold belt structures. Journal of Structural Geology 24, 173–192.

Lee, Y.H., Hsieh, M.-L., Lu, S.-D., Shih, T.-S., Wu, W.-Y., Sugiyama, Y., Azuma, T., Kariyae, Y., 2003. Slip vectors of the surface rupture of the 1999 Chi-Chi earthquake, western Taiwan. Journal of Structural Geology 25, 1917–1931.

Liesa, C.L., Lisle, R.J., 2004. Reliability of methods to separate stress tensors from heterogeneous fault-slip data. Journal of Structural Geology 26, 559–572.

Mojena, R., 1977. Hierarchical grouping methods and stopping rules: an evaluation. The Computer Journal 29, 359–363.

Nemcok, M., Lisle, R.J., 1995. A stress inversion procedure for polyphase fault/slip data sets. Journal of Structural Geology 17, 1445–1453.

Orife, T., Lisle, R.J., 2003. Numerical processing of palaeostress results. Journal of Structural Geology 25 (6), 949–957.

Price, R.A., 1988. The mechanical paradox of large thrusts. Geological Society of America Bulletin 100, 1898–1908.

Ramsay, J.G., Lisle, R.J., 2000. The Techniques of Modern Structural Geology Volume 3: Applications of Continuum Mechanics in Structural Geology. Academic Press, London. 346 pp.

Sato, K., Yamaji, A., 2006a. Embedding stress difference in parameter space for stress tensor inversion. Journal of Structural Geology 28, 957–971.

Sato, K., Yamaji, A., 2006b. Uniform distribution of points on a hypersphere for improving the resolution of stress tensor inversion. Journal of Structural Geology 28, 972–979.

Shan, Y., Fry, N., 2005. A hierarchical cluster approach for forward separation of heterogeneous fault/slip data into subsets. Journal of Structural Geology 27, 929–936.

Shan, Y., Suen, H., Lin, G., 2003. Separation of polyphase fault/slip data: an objective-function algorithm based on hard division. Journal of Structural Geology 25, 829–840.

Shan, Y., Li, Z., Lin, G., 2004. A stress inversion procedure for automatic recognition of polyphase fault/slip data sets. Journal of Structural Geology 16, 919–925.

Shan, Y., Liu, L., Peng, S., 2006. Discrimination of two planar structures in directional data. Mathematical Geology 38, 375–388.

Xie, F.R., Liu, G.X., 1989. Analysis of neotectonic stress field in area of the central segment of Altun fault zone, China. Earthquake Research in China 1, 26–36 (in Chinese with an English abstract).

Xu, P., 2004. Determination of regional stress tensors from fault-slip data. Geophysical Journal International 157, 1316–1330.

Yamaji, A., 2000. The multiple inverse method: a new technique to separate stresses from heterogeneous fault-slip data. Journal of Structural Geology 22, 441–452.